ADVANCED THEORY AND SIMULATIONS
www.advtheorysimul.com

2D Nitrogen-Containing Carbon Material C_5N as Potential Host Material for Lithium Polysulfides: A First-Principles Study

Dandan Wang, Haibo Li, Liangliang Zhang,* Zhonghui Sun, DongXue Han, Li Niu, and Jialong Zhao*

Two-dimensional (2D) materials are identified to be efficient in many applications. In this work, a novel 2D nitrogen-containing carbon material, C_5N, is theoretically designed through structure changes in atomic scale, that is, introducing V_C–V_N bivacancy defects along lines in perfect C_3N monolayer. C_5N monolayer is verified to be chemically, mechanically, dynamically, and thermodynamically stable based on cohesive energy, elastic constants, phonon spectrum, and molecular dynamics calculations. C_5N is determined to be metallic which is an important property for battery electrode. Moreover, the anchoring performance of S_8 and Li_2S_n (n = 1, 2, 4, 6, and 8) on C_5N monolayer and the anchoring mechanisms are explored. The adsorption energies are calculated to be −0.24, −1.20, −1.10, −1.06, −1.63, and −1.59 eV for S_8, Li_2S_8, Li_2S_6, Li_2S_4, Li_2S_2, and Li_2S, respectively. The anchoring effect of Li_2S_n on C_5N monolayer originates from the charge transfer between lithium polysulfides and C_5N surface. These results reveal that C_5N monolayer is a promising host material for polysulfides in Li–S batteries. Our calculations illustrate the design of nanostructures and facilitate the application of carbon-based 2D materials in environment and energy.

1. Introduction

2D materials have attracted great attention and have been applied extensively in energy storage aspects due to their unique physical and chemical properties.[1–4] Among them, carbon-based 2D materials have always been the research focus. For example, as the ancestor of 2D materials, graphene has been extensively studied on both experiment and theory and has been successfully applied in nanoelectronics, environmental, and energy storage devices.[5–7] C_3N_4, a classic nanoporous graphitic carbon nitride which could be easily synthesized from urea,[8] possesses excellent physical and chemical stability and appealing electronic properties with a band gap of 2.70 eV.[9] It has attracted a lot of attention and has been demonstrated to be well suited for photosynthesis,[10] lithium–sulfur batteries,[11] and other applications. What is more, boron–carbon honeycomb structure, BC_3 monolayer, has also been successfully obtained experimentally.[12,13] Liu et al. demonstrated that layered BC_3 possesses outstanding Li storage capacity, which is about twice as large as that of graphite.[14] Recently, Qie et al. reported that BC_3 monolayer shows good anchoring performance for lithium polysulfides, indicating that BC_3 could be an appropriate cathode material for Li–S batteries.[15]

However, carbon-based 2D materials need to be modulated and modified for better performances in real applications. Many approaches have been developed to improve their properties, including element doping, vacancy defect regulation,

Dr. D. D. Wang, Prof. H. B. Li, Prof. J. L. Zhao
Key Laboratory of Functional Materials Physics and Chemistry of the Ministry of Education
Jilin Normal University
Changchun 130103, China
E-mail: lihaibo@jlnu.edu.cn
Dr. L. L. Zhang
State Key Laboratory of Luminescence and Applications
Changchun Institute of Optics
Fine Mechanics and Physics
Chinese Academy of Sciences
3888 Eastern South Lake Road, Changchun 130103, China
E-mail: zhangliangliang@ciomp.ac.cn
Dr. Z. H. Sun, Prof. D. X. Han, Prof. L. Niu
Center for Advanced Analytical Science
School of Chemistry and Chemical Engineering
Guangzhou University
Guangzhou 510006, China
Prof. D. X. Han, Prof. L. Niu
State Key Laboratory of Electroanalytical Chemistry
Engineering Laboratory for Modern Analytical Techniques
Changchun Institute of Applied Chemistry
Chinese Academy of Science
Changchun 130022, China

The ORCID identification number(s) for the author(s) of this article can be found under https://doi.org/10.1002/adts.201800165

DOI: 10.1002/adts.201800165

hydrogenation, and even external strain strategy. For example, saturation of sp^2 bonds in graphene by hydrogen atoms would result in graphane, which has been demonstrated to be a semiconductor appropriate as channel material in field effect transistors and photocatalysts, etc.[16] Tao et al. fabricated a N and P dual-doped carbon fibers/graphitic carbon nitride (*hu*CP/g-C_3N_4) which was used as ultrahigh capacity and rate anode for Li and Na ion batteries.[17] To enhance the conductivity and improve the electrochemical performance of C_3N_4, magnesiothermic denitriding technology was used by Chen et al. to reduce the graphitic nitrogen of C_3N_4, and the obtained nitrogen-deficient C_3N_4 showed enhanced performance for Li ion batteries.[18] Jia et al. have also demonstrated that the defects derived by the removal of heteroatoms from graphene are advantageous for all three basic electrochemical reactions, such as oxygen reduction, oxygen evolution, and hydrogen evolution reactions.[19] In the recent 2 years, Wu et al. have designed several 2D cathodes for Li–S batteries with excellent performance,[20–22] especially the ultrathin layered $MoSe_2$ with enriched edge sites and theoretical calculations confirmed that lithium polysulfides prefer to adsorb on the edge sites.[23]

Recently, Yang et al. synthesized a novel flat 2D crystal, C_3N, in which the nitrogen atoms are evenly distributed and no holes exist.[24] In our previous work, we have investigated the effect of strain and hydrogenation on the properties of C_3N and concluded that strained and hydrogenated C_3N monolayers are promising candidate material for future applications in the applications of Li ion batteries and photocatalysts.[25] In this work, we first introduced a "$V_C + V_N$" bivacancy in C_3N monolayer, after full structure optimization, the "$V_C + V_N$" bivacancy evolved into a new configuration consisting of "5 carbon nitrogen ring-8 carbon nitrogen ring-5 carbon ring" (5CN-8CN-5C) (shown in Figure S1b, Supporting Information). Stimulated by the defect evolution caused by structure optimization, we studied an extreme case more deeply, in which numerous "$V_C + V_N$" bivacancy line defects were intoduced through omiting the neighbor lattice C and N atoms from C3N monolayer (Figure S1c, Supporting Information). Encouragingly, a novel 2D carbon nitride compound, C_5N in stoichiometry and composed of 5CN-8CN-5C rings, was discovered. Based on density functional theory (DFT) calculations, the novel 2D crystal, C_5N, has chemical, mechanical, dynamic, and thermodynamic stability. Accurate electronic structures obtained by Heyd–Scuseria–Ernzerhof (HSE06) functional calculations indicate that C_5N monolayer is metallic. Moreover, we also employ systematic DFT calculations to study the anchoring performance of S_8 and Li_2S_n ($n = 1, 2, 4, 6, 8$) on C_5N surface. The adsorption energies and transfer charges between Li_2S_n and 2D monolayer imply that the C_5N monolayer is a promising host material for Li_2S_n in Li–S batteries.

2. Experimental Section

We performed all first-principles calculations based on DFT[26] using the projected augmented wave (PAW) method[27] which was implemented in the Vienna ab initio simulation package (VASP). To compute the electron exchange–correlation energy, the Perdew–Burke–Ernzerhof (PBE) generalized gradient approximation[28,29] was used. In addition, the HSE06 functional[30] was applied to acquire accurate electronic band structures and density of states (DOS) of C_5N monolayer. The long-range vdW interactions were taken into consideration by using DFT-D2 correction method of Grimme.[31] The cutoff energy for the plane wave basis set is 450 eV. The optimized geometries were obtained with all the atomic positions relaxed until their residual forces are less than 0.01 eV $Å^{-1}$. To avoid interaction between two adjacent periodic images, a 20 Å vacuum space perpendicular to the monolayer plane was adopted. In this work, different Monkhorst–Pack K-point samplings for the Brillouin-zone integration were set for different calculations. The $3 \times 3 \times 1$ K-points were applied for the structure optimization of Figure S1a,c, Supporting Information. For calculations involved in C_5N unit cell, the K-point samplings were set as $1 \times 5 \times 3$ and $1 \times 14 \times 6$ to calculate its structure properties and DOS, respectively. For the adsorption systems, the K-point samplings were set as $1 \times 2 \times 2$ and $1 \times 3 \times 3$ for structure optimization and DOS calculations, respectively. Density-functional perturbation theory (DFPT)[32,33] was used to calculate the phonon dispersion properties. Through first-principles molecular dynamics (MD) calculations,[34] we assessed the thermodynamic stability of C_5N monolayer. The MD calculations in NVT ensemble lasted for 10 ps with a time step of 1.0 fs and the temperature was controlled by Nosé–Hoover method.[35]

To investigate the anchoring effect of 2D material toward Li_2S_n, the adsorption energy E_{ads} of Li_2S_n on surface was calculated according to the equation of $E_{ads} = E_{surface} + E_{Li2Sn} - E_{system}$, where E_{system}, $E_{surface}$, and E_{Li2Sn} were the total energy of the 2D material with Li_2S_n adsorbed on it, the total energy of pristine 2D material, and the total energy of isolated Li_2S_n, respectively. According to this definition, the more positive the E_{ads}, the stronger the adsorption. Partial density of states (PDOS) of adsorbed systems have also been calculated to study the adsorption effect. For adsorbed systems, the DOS calculations were based on PBE functional instead of HSE06 functional in order to save calculation cost. In addition, charge density difference calculations and Bader charge analysis have been made to study the charge transfer between the 2D material and Li_2S_n.

3. Results and Discussion

3.1. Structure and Electronic Properties of C_5N Monolayer

The unrelaxed structure of C_3N with "$V_C + V_N$" bivacancy line defects is constructed through removing the nearest neighbor C and N atoms from C_3N monolayer which is in *xy* plane as shown in Figure S1c, Supporting Information. Interestingly, after fully optimization the nanoarchitecture is composed of 5CN–8CN–5C rings. By imposing symmetry on the optimized structure, the defected monolayer is transfer into *yz* plane, as shown in **Figure 1**a. Considering the atomic ratio in the defected monolayer, its chemical formula can be regarded as C_5N, which is a brand new carbon nitrogen ratio for 2D nitrogen-containing carbon materials. In each unit cell of C_5N monolayer, there are ten C atoms and two N atoms with AMM2 symmetry and the calculated equilibrium lattice parameters are b = 3.645 Å and c = 8.896 Å. The corresponding bond lengths of C–C and C–N bonds are listed in **Table 1**. Based on the definition of cohesive energy: $E_{coh} = (nE_C +$

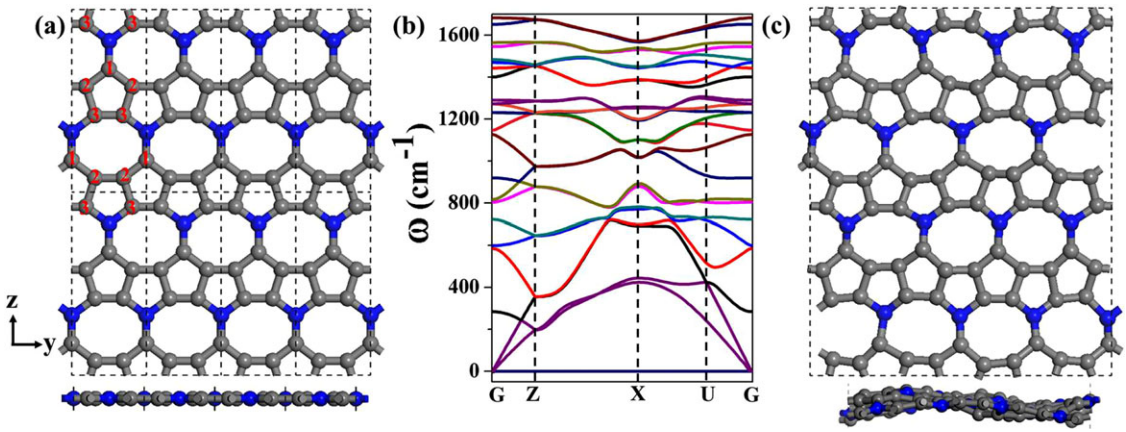

Figure 1. a) Top (upper) and side (lower) view of the atomic structure of C_5N monolayer. The gray and blue balls represent C atoms and N atoms, respectively. Every parallelogram of the dotted line including ten C atoms and two N atoms signifies the unit cell. b) Phonon dispersion plots along high symmetry directions in the first Brillouin zone (BZ) of C_5N monolayer. c) Top (upper) and side (lower) views of snapshots of the C_5N monolayer equilibrium structures at the end of 10 ps MD calculation under 1000 K.

Table 1. The corresponding bond lengths in C_5N monolayer. The integers shown in 1a indicate C_i ($i = 1, 2, 3$).

Bond	C_1–N	C_3–N	C_1–C_2	C_2–C_3	C_2–C_2	C_3–C_3
Bond length [Å]	1.373	1.401	1.412	1.461	1.387	1.391

$mE_N - E_{C5N})/(m+n)$, where E_C, E_N, and E_{CN} are the total energies of a single C atom, a single N atom, and C_5N monolayer, m and n are the number of C and N atoms in the supercell, respectively. The E_{coh} of C_5N monolayer is 8.22 eV per atom, higher than that of graphene (7.95 eV per atom),[36] indicating the strong chemical bonds in the 2D compound.

To evaluate the mechanical stability of C_5N, its elastic constants were calculated. The calculated results of C_{11} = 17.77 N m^{-1}, C_{12} = 3.27 N m^{-1}, C_{22} = 388.11 N m^{-1}, and C_{66} = 3.35 N m^{-1} satisfy the mechanical stability criteria of 2D material, that is $C_{11}C_{22} - C_{12}^2 > 0$ and $C_{66} > 0$.[37] The phonon dispersions were investigated based on DFPT and the phonon dispersion plots are given in Figure 1b. The kinetic stability of C_5N monolayer was verified by the fact that no appreciable imaginary frequencies exist in the phonon dispersion curves. The highest phonon frequency at G point is 1682.07 cm^{-1} and the corresponding Debye temperature is 2421 K, a little higher than those of C_3N due to the relative stronger bonds of C_1–N, C_3–N, C_2–C_2, and C_3–C_3.[25] Moreover, the thermodynamic stability of C_5N was assessed through first-principles MD calculations, in which a 4 × 2 supercell was employed. MD results reveal that the structure remains its lattice construction at 300 K for 10 ps (not shown here) while distortion appears at 1000 K (Figure 1c), which means that C_5N is thermally stable at room temperature and its melting point is higher than 1000 K.

The calculated electronic band structure and DOS based on HSE06 calculations for C_5N are shown in **Figure 2**. Interestingly, the Fermi energy locates well below the valence-band maximum and the band gap structure is similar to that of Cu metal,[38] meaning that C_5N monolayer has significant electrical conductivity and metallic characteristic. Moreover, DOS peaks around the Fermi energy mainly originated from the electrons of C atoms.

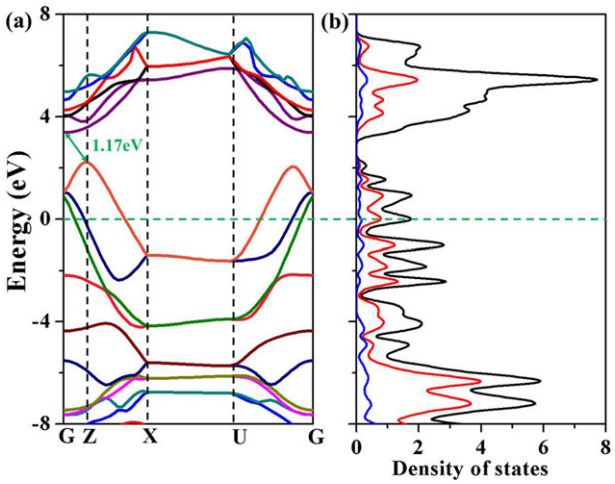

Figure 2. a) Band structure and b) density of states (DOS) of C_5N monolayer obtained from HSE06 calculations. For reference, the Fermi level is set at 0 eV. In (b), the black, red, and blue lines denote the total DOS of C_5N, the partial DOS of C atoms, and the partial DOS of N atoms, respectively.

3.2. The Anchoring Performance of Li_2S_n (x = 1, 2, 4, 6, 8) on C_5N Surface

With the development of synthetic and testing technology, 2D materials have attracted great attention in the applications of Li–S batteries, in which the 2D materials with high theoretical surface areas and unique electronic properties serve as host materials for lithium polysulfides Li_2S_n (n = 1, 2, 4, 6, 8). In this work, the promising application of C_5N as a host material in Li–S batteries has been investigated. Before investigation of Li_2S_n adsorption properties on C_5N, we firstly relaxed the structures of Li_2S_n, whose optimized structures are shown in **Figure 3**. The calculated 3D geometries and corresponding bond lengths are in accordance with the previous reports.[15] Then we studied systematically the adsorption configurations of Li_2S_n

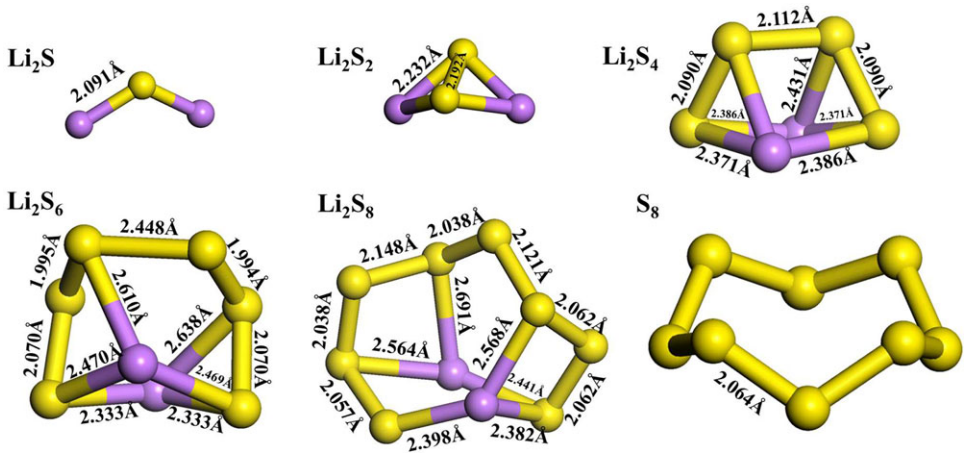

Figure 3. The optimized structures of Li_2S, Li_2S_2, Li_2S_4, Li_2S_6, Li_2S_8, and S_8. The purple and yellow balls represent Li and S atoms, respectively.

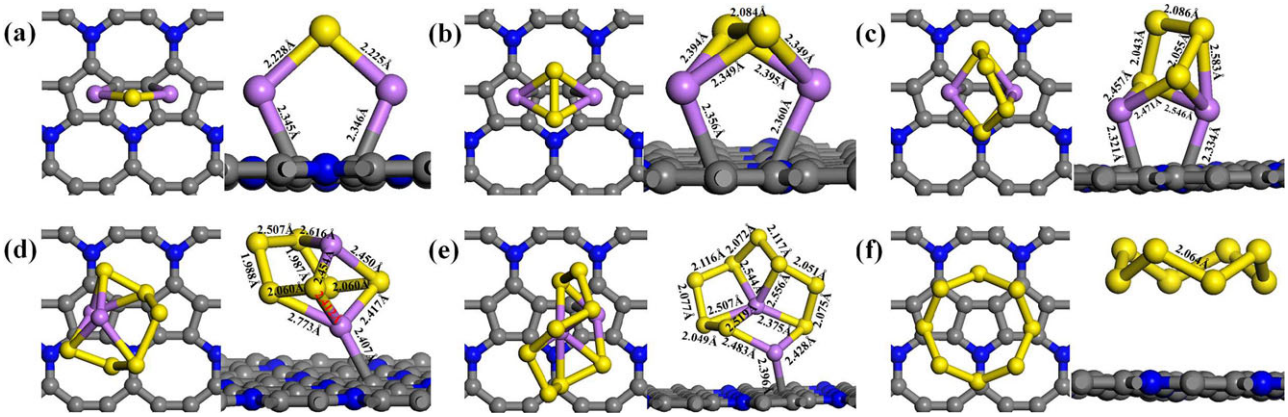

Figure 4. The most stable adsorption configuration of a) Li_2S, b) Li_2S_2, c) Li_2S_4, d) Li_2S_6, e) Li_2S_8, and f) S_8 on C_5N surface. The purple, yellow, gray, and blue balls represent Li, S, C, and N atoms, respectively.

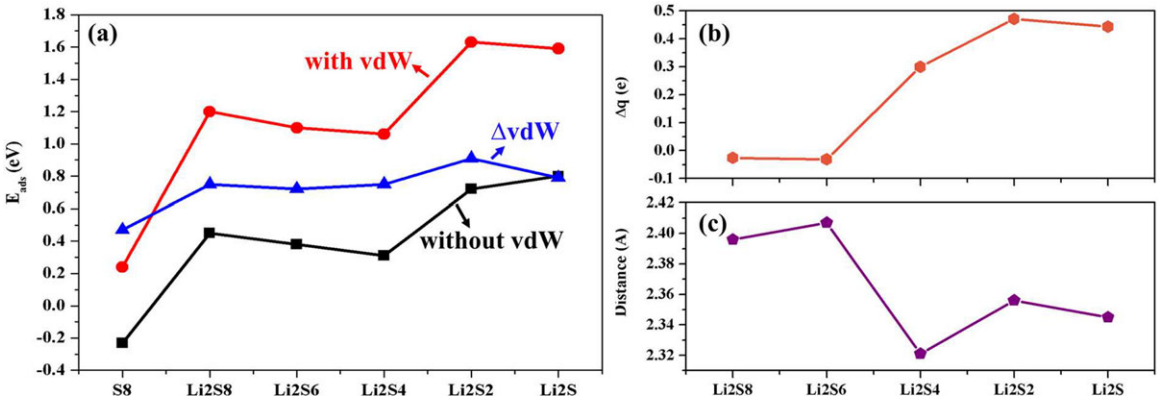

Figure 5. a) Adsorption energies for Li_2S_n on C_5N. Black and red curves represent using the simulation method without and with vdW functional. Blue curve represents the strength of vdW physical interaction. b) The shortest distance between Li atom of Li_2S_n and C/N atom of C_5N surface. c) The quantity of transferred charge from Li_2S_n to C_5N surface (Δq) during the lithium process.

toward C_5N surface. The most stable adsorption configurations are shown in **Figure 4** and the corresponding adsorption energy profile during the lithium process is presented in **Figure 5**a.

As shown in Figure 4a,b, for Li_2S and Li_2S_2, their two Li atoms are located at the hollow center sites of two 5-carbon rings and Li atoms bind with the C atoms of C_5N surface with the corresponding bond lengths between 2.34 and 2.36 Å. The two Li atoms of

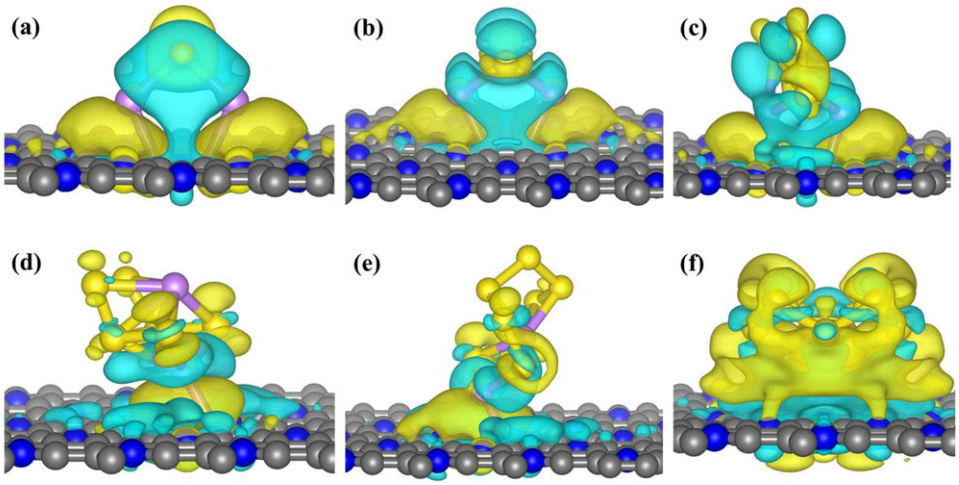

Figure 6. The isosurfaces of charge density difference of a) Li_2S, b) Li_2S_2, c) Li_2S_4, d) Li_2S_6, e) Li_2S_8, and f) S_8 adsorbed on C_5N surface with the isovalue of 0.003 $Å^{-3}$. The blue wireframes denote loss of electrons and yellow wireframes denote gain of electrons.

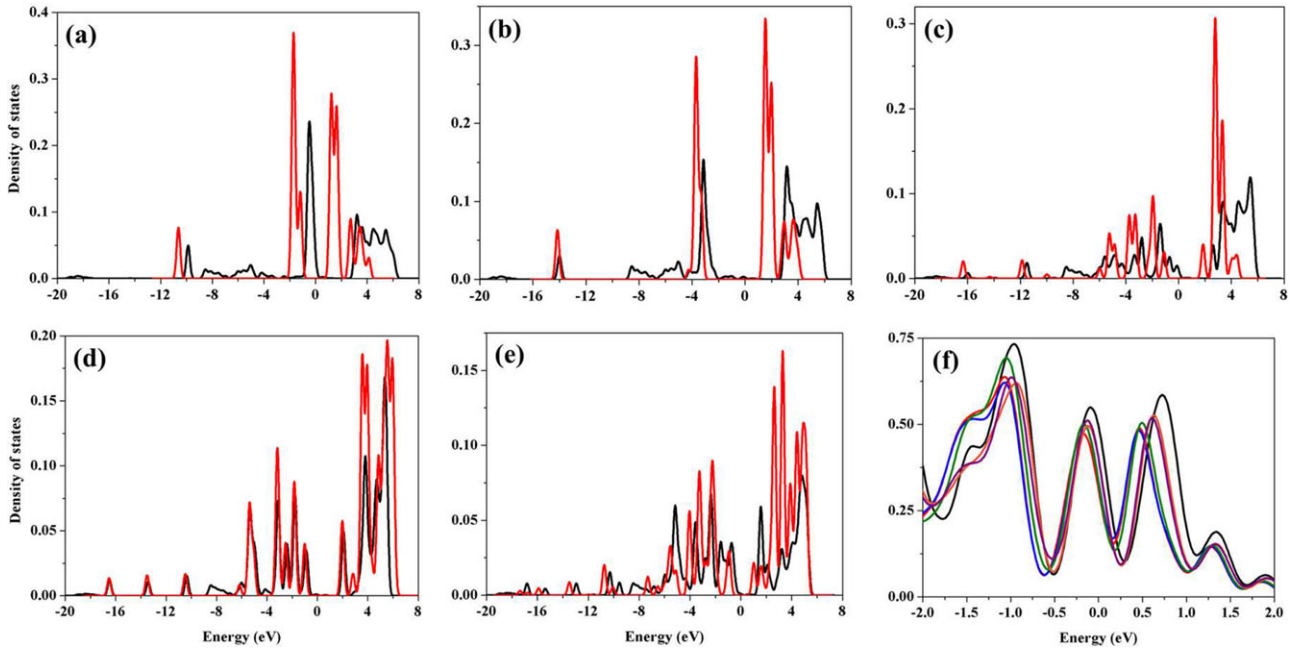

Figure 7. The partial density of states (PDOS) of the Li atom before and after adsorbed on C_5N surface: a) Li_2S, b) Li_2S_2, c) Li_2S_4, d) Li_2S_6, and e) Li_2S_8. f) The PDOS of the C atoms of 5-carbon ring whose hollow site is located by Li atom. In (a–e), the red and black lines denote the PDOS of Li atom before and after Li_2S_n adsorption on C_5N surface, respectively. In (f), the black, red, blue, green, orange, and purple lines represent the PDOS of the C atoms of 5-carbon ring without adsorption, with Li_2S, Li_2S_2, Li_2S_4, Li_2S_6, and Li_2S_8 adsorption, respectively.

Li_2S_4 locate at the positions offset from the hollow center of the 5-carbon rings and the corresponding Li-C bond lengths are 2.321 and 2.334 Å. For long-chain clusters, Li_2S_6 and Li_2S_8, one of their Li atoms is located at the hollow center site of a 5-carbon ring of C_5N surface and the Li–C bond lengths are around 2.40 Å. The Li–C distance variation is shown in Figure 5c and the non-monotonicity may originate from the synergistic effect of chemical and vdW physical interaction. For S_8, the adsorption energy is only 0.24 eV, indicating the physical adsorption of S_8 on C_5N surface. What is more, Li_2S_n can also anchor on the surface with the Li atoms located at the hollow center sites of 5-carbon–nitrogen rings (Figure S2, Supporting Information) with the adsorption energies a little bit lower (about 0.15 eV lower) than those of the corresponding adsorption configurations shown in Figure 4. As reported, the adsorption energies are only −0.74, −0.80, −0.73, −0.99, and −1.11 eV for Li_2S, Li_2S_2, Li_2S_4, Li_2S_6, and Li_2S_8 on the pristine C_3N surface and the C_3N monolayer is inadequate to act as anchoring material for Li_2S_n in Li–S batteries.[14] Comparing the adsorption energies of Li_2S_n clusters on C_5N and C_3N, C_5N surface can bind Li_2S_n more strongly, indicating that C_5N is a promising anchoring material for Li_2S_n and defect regulation is a very effective strategy to improve materials' performance. The

improvement in adsorption properties may have originated from the specific geometric construction and electronic properties of C_5N in comparison with C_3N.

Moreover, adsorption energy calculations without vdW effects have also been performed to estimate the contributions by chemical interaction and vdW physical interaction. The strength of vdW physical interaction is derived as $\Delta vdW = E_{ads}$ (vdW) $- E_{ads}$(without vdW). Figure 5a presents the adsorption energy profiles with Li_2S_n. For S8 cluster, the vdW physical interaction is the decisive factor that leads to its anchoring effect on C_5N surface. The physical interaction is slightly stronger than the chemical interaction for long-chain Li_2S_n ($n = 8, 6, 4$) while the opposite happens for Li_2S_2 and Li_2S, resulting that the total interaction is not monotonous with the increase of S elements and the adsorption strength decreases to 1.06 eV at the middle stage (Li_2S_4).

To understand the anchoring mechanism of Li_2S_n on C_5N surface, we calculated the charge density difference that originated from adsorption and made Bader charge analysis. As can be seen from the charge density difference plots in **Figure 6**, there are obvious charge transfers from Li_2S_n ($n = 1, 2, 4$) to C_5N surface and the net transferred charges are 0.444e, 0.471e, and 0.300e, respectively. While for Li_2S_6 and Li_2S_8, the net charge transfer is from C_5N surface to Li_2S_n cluster, with the quantity of −0.031e and −0.026e. The variation of the transferred charge follows the similar trend with the chemical interaction, as shown in Figure 5b. The charge is also transferred from C_5N surface to S8 cluster and the quantity is −0.036e.

For further understanding of the interaction between surface and Li_2S_n, PDOS calculations for C_5N and Li_2S_n before and after adsorption have been performed. The PDOS plots of Li atoms of Li_2S_n are shown in **Figure 7**a–e and Figure 7f gives the PDOS for C atoms of the 5-carbon rings whose hollow center sites are occupied by Li atoms. Obviously, after adsorption for Li_2S_n ($n = 1, 2, 4$), the PDOS of Li atoms are broadly dispersed. While for Li_2S_6 and Li_2S_8, the dispersion of Li PDOS is slightly broadened after adsorption. These results reveal that interaction occurs between surface C atoms and Li atoms of Li_2S_n. Moreover, comparing the peaks of PDOS presented in Figure 7f, the ratio of the peaks for C atoms near Fermi level (about −0.2 eV) increase after Li_2S_n adsorption, which is the result of electron transfer. These PDOS results indicate the electron density redistribution after adsorption, in agreement with charge density difference and Bader charge analysis.

4. Conclusions

In summary, motivated by defected C_3N with bivacancy, we have designed a new 2D nitrogen-containing carbon nitride, that is C_5N, a brand new carbon nitrogen ratio for 2D nitrogen-containing carbon materials. Based on DFT and HSE06 calculations, C_5N is identified to possess metallic characteristic. The 2D novel structure of C_5N makes it a promising anchoring material for Li_2S_n ($n = 1, 2, 4, 6, 8$) in Li–S batteries. The adsorption energies are calculated to be −1.59, −1.63, −1.06, −1.10, and −1.20 eV for Li_2S, Li_2S_2, Li_2S_4, Li_2S_6, and Li_2S_8 on C_5N surface, respectively, indicating that the C_5N surface could bind Li_2S_n clusters more strongly than pristine C_3N, which is essential for good cycle life and coulomb efficiency in Li–S batteries. Our results reveal that the novel 2D material C_5N could be a promising material in wide applications involved in environment and energy.

Supporting Information

Supporting Information is available from the Wiley Online Library or from the author.

Acknowledgements

This work was supported by NSFC, China (11604330, 21622509, 21475122, and 21527806), Department of Science and Techniques of Jilin Province (20160201008GX), Jilin Province Development and Reform Commission, (2016C014 and 2017C053-1), Science and Technology Bureau of Changchun (15SS05).

Conflict of Interest

The authors declare no conflict of interest.

Keywords

2D nitrogen-containing carbon material, density functional theory calculations, lithium polysulfides adsorption

Received: October 22, 2018
Revised: November 21, 2018
Published online:

[1] X. Y. Zhang, S. H. Sun, X. J. Sun, Y. R. Zhao, L. Chen, Y. Yang, W. Lu, D. B. Li, *Light: Sci. Appl.* **2016**, *5*, e16130.
[2] M. Autore, P. Li, I. Dolado, F. J. Alfaro-Mozaz, R. Esteban, A. Atxabal, F. Casanova, L. E. Hueso, P. Alonso-González, J. Aizpurua, A. Y. Nikitin, S. Vélez, R. Hillenbrand, *Light: Sci. Appl.* **2018**, *7*, 17172.
[3] Q. Tang, Z. Zhou, P. Shen, *J. Am. Chem. Soc.* **2012**, *134*, 16909.
[4] J. Kibsgarrd, Z. B. Chen, B. N. Reinecke, T. F. Jaramillo, *Nat. Mater.* **2012**, *11*, 963.
[5] V. Apalkov, M. I. Stockman, *Light: Sci. Appl.* **2014**, *3*, e191.
[6] W. Chartarrayawadee, S. E. Moulton, D. Li, C. O. Too, G. C. Wallace, *Electrochim. Acta* **2012**, *60*, 213.
[7] H. Chen, C. Chen, Y. J. Liu, X. L. Zhao, N. Ananth, B. Zheng, L. Peng, T. Huang, W. Gao, C. Gao, *Adv. Energy Mater.* **2017**, *7*, 1700051.
[8] X.-X. Zou, G.-D. Li, Y.-N. Wang, J. Zhao, C. Yan, M.-Y. Guo, L. Li, J.-S. Chen, *Chem. Commun.* **2011**, *47*, 1066.
[9] J. Liu, W. Li, L. Duan, X. Li, L. Ji, Z. Geng, K. Huang, L. Lu, L. Zhou, Z. Liu, *Nano Lett.* **2015**, *15*, 5137.
[10] L. H. Lu, Z. Z. Lv, Y. J. Si, M. Y. Liu, S. Zhang, *Appl. Surf. Sci.* **2018**, *462*, 693.
[11] Z. Meng, Y. Xie, T. W. Cai, Z. X. Sun, K. Jiang, W.-Q. Han, *Electrochim. Acta* **2016**, *210*, 829.
[12] H. Tanakaa, Y. Kawamataa, H. Simizua, T. Fujitaa, H. Yanagisawa, S. Otanic, C. Oshima, *Solid State Commun.* **2005**, *136*, 22.
[13] A. Ueno, T. Fujita, M. Matsue, H. Yanagisawa, C. Oshima, F. Patthey, *Surf. Sci.* **2006**, *600*, 3518.
[14] Y. Liu, V. I. Artyukhov, M. Liu, A. R. Harutyunyan, B. I. Yakobson, *J. Phys. Chem. Lett.* **2013**, *4*, 1737.

[15] Y. Qie, J. Liu, S. Wang, S. Gong, Q. Sun, *Carbon* **2018**, *129*, 38.
[16] M. Pumera, C. H. A. Wong, *Chem. Soc. Rev.* **2013**, *42*, 5987.
[17] H. C. Tao, L. Y. Xiong, S. L. Du, Y. Q. Zhang, X. L. Yang, L. L. Zhang,. *Carbon* **2017**, *122*, 54.
[18] J. J. Chen, Z. Mao, L. Zhang, D. Wang, Y. Xu, L. Bie, B. D. Fahlman, *ACS Nano* **2017**, *11*, 12650.
[19] Y. Jia, L. Z. Zhang, A. J. Du, G. P. Gao, J. Chen, X. C. Yan, C. L. Brown, X. D. Yao, *Adv. Mater.* **2016**, *28*, 9532.
[20] S.Y. Liu, C. Y. Fan, Y. H. Shi, H. C. Wang, X. L. Wu, J. P. Zhang, *ACS Appl. Mater. Interfaces* **2018**, *10*, 509.
[21] C. Y. Fan, S.Y. Liu, H. H. Liu, H. F. Wang, H. C. Wang, X. L. Wu, H. Z. Sun, J. P. Zhang, *ACS Appl. Mater. Interfaces* **2016**, *8*, 28689.
[22] C. Y. Fan, S.Y. Liu, H. H. Liu, Y. H. Shi, H. C. Wang, H. F.Wang, H. Z. Sun, X. L. Wu, J. P. Zhang, *J. Mater. Chem. A* **2017**, *5*, 11255.
[23] C. Y. Fan, Y. P. Zheng, X. H. Zhang, Y. H. Shi, S. Y. Liu, H. C. Wang, X. L. Wu, H. Z. Sun, J. P. Zhang, *Adv. Energy Mater.* **2018**, *8*, 1703638.
[24] S. W. Yang, W. Li, C. C. Ye, G. Wang, H. Tian, C. Zhu, P. He, G. Q. Ding, X. M. Xie, Y. Liu, Y. Lifshitz, S.-T. Lee, Z. H. Kang, M. H. Jiang, *Adv. Mater.* **2017**, *29*, 1605625.
[25] D. D. Wang, Y. Bao, T. S. Wu, S. Y. Gan, D. X. Han, L. Niu, *Carbon* **2018**, *134*, 22.
[26] P. Hohenberg, K. Walter, *Phys. Rev.* **1964**, *136*, B864.
[27] G. Kresse, D. Joubert, *Phys. Rev. B* **1999**, *59*, 1758.
[28] J. P. Perdew, K. Burke, M. Ernzerhof, *Phys. Rev. Lett.* **1996**, *77*, 3865.
[29] S. Grimme, *J. Comput. Chem.* **2006**, *27*, 1787.
[30] J. Paier, M. Marsman, K. Hummer, G. Kresse, I. C. Gerber, J. G. Ángyán, *J. Chem. Phys.* **2006**, *124*,154709.
[31] S. Grimme, *J. Comput. Chem.* **2006**, *27*, 1787.
[32] S. Baroni, P. Giannozzi, A. Testa, *Phys. Rev. Lett.* **1987**, *58*, 1861.
[33] X. Gonze, *Phys. Rev. A* **1995**, *52*, 1086.
[34] M. C. Payne, M. P. Teter, D. C. Allan, T. A. Arias, J. D. Joannopoulos, *Rev. Mod. Phys.* **1992**, *64*, 1045.
[35] G. J. Martyna, M. L. Klein, M. E. Tuckerman, *J. Chem. Phys.* **1992**, *97*, 2635.
[36] Y. F. Li, Y. L. Liao, Z. F. Chen, *Angew. Chem., Int. Ed.* **2014**, *53*, 7248.
[37] Y. Ding, Y. Wang, *J. Phys. Chem. C* **2013**, *117*, 18266.
[38] W. D. Callister, Jr., *Fundamentals of Materials Science and Engineering*, John Wiley & Sons, New York **2001**.